Pyrochlore supergroup minerals from the alkaline pegmatites in the Larvik Plutonic Complex, southern Norway

Paula C. Piilonen, Glenn Poirier, Ralph Rowe & Alf Olav Larsen

Introduction

Pyrochlore supergroup minerals are ubiquitous phases within all alkaline pegmatites in the Larvik Plutonic Complex, Oslo rift, southern Norway. It was first discovered in the 1820's by N.O. Tank from a locality near Stavern, Larvik, Vestfold, and was described in 1826 by Wöhler. Pyrochlore was the second mineral to be described as a new species from the alkaline pegmatites of the Larvik Plutonic Complex, next to zirconolite (*polymignite*). It is one of the earliest minerals to crystallize in the alkaline pegmatites, and occurs dominantly as subhedral to anhedral yellow, orange and reddish-orange to dark red-brown grains up to 1 cm in width embedded in perthitic feldspar, amphibole, aegirine, magnetite and zircon. Primary, euhedral octahedra up to 2-4 cm have been found at Stavern (Larvik, Vestfold; Fig. 1) and Stokkøya (Langesundsfjord). The majority of these pyrochlore supergroup minerals are metamict and have undergone extensive alteration. Late-stage euhedral crystals of pyrochlore, most only a few mm's across, are often late-stage phases, found crystallizing on acicular aegirine in the agpaitic pegmatites at Lysebo (Hedrum). Pyrochlore supergroup minerals have only rarely been found in the agpaitic pegmatites in ring sections 9 and 10; perovskite-group minerals are the common Nb-oxide phase.

Fig. 1. Pyrochlore crystal from the Håkestad quarry, Tjølling, Larvik, collected in June 2000. The crystal is 10 mm along the edge. Collection and photo A.O. Larsen.

In an effort to shed light on the geological, geochemical and mineralogical processes that have collectively contributed to the formation and evolution of the alkaline pegmatites of the Larvik Plutonic Complex, a series of studies have been undertaken on the rock-forming and important accessory minerals. Being a primary, ubiquitous magmatic phase, pyrochlore supergroup minerals allow us to determine the high field-strength element characteristics of the magma from which the pegmatite formed. In addition, the susceptibility of pyrochlore supergroup minerals to post-magmatic and post-metamictization alteration by fluids allows for determination of the composition of the hydrothermal and meteoritic fluids which infiltrated the pegmatites following crystallization.

Primary pyrochlore supergroup minerals were sampled from 26 alkaline pegmatites across the Larvik Plutonic Complex (Table 1, Fig. 2) in order to determine their chemical composition and examine their alteration patterns. Species names were applied to each specimen in accordance with the new pyrochlore supergroup nomenclature proposed by the IMA (Atencio et al. 2010).

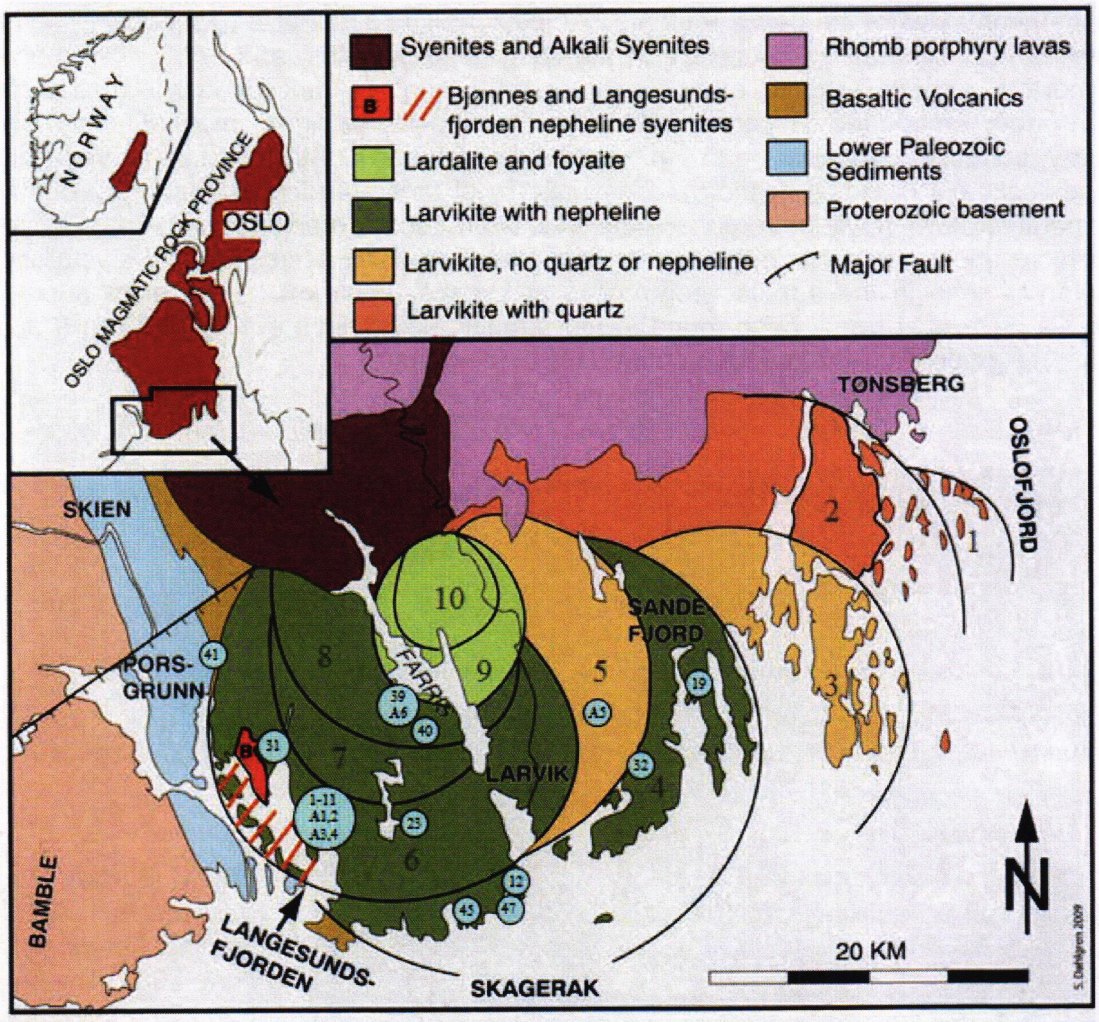

Fig. 2. The Larvik Plutonic Complex (LPC) showing the 10 ring sections (RS) and pyrochlore supergroup sample locations. The oldest RS occur in the east and are miaskitic. Younger plutons have intruded successively westward, becoming increasingly peralkaline. From Dahlgren (2010), modified from Petersen (1978).

Chemical composition

Chemical analyses of pyrochlore supergroup minerals were done with a JEOL Superprobe 8230 at the University of Ottawa. Operating conditions were as follows: beam diameter of 5 μm, operating voltage 40 kV, and a beam current of 11 nA. A total of 29 elements were sought and the following standards and *X*-ray lines were employed: synthetic diopside (Si *K*α, Mg *K*α, Ca *K*α), sanidine (K *K*α, Al *K*α,), rutile (Ti *K*α), VP_2O_7 (V *K*α), synthetic $CePO_4$ (Ce *L*α), Mn-columbite (Nb *L*α, Mn *K*α), synthetic $LaPO_4$ (La *L*α), synthetic $NdPO_4$ (Nd *L*α), synthetic $SmPO_4$ (Sm *L*α), synthetic $PrPO_4$ (Pr *L*α), synthetic YIG garnet (Y *L*α), zircon (Zr *L*α), hematite (Fe *K*α), celestine (Sr *L*β, S *K*α), microlite (F *K*α, Na *K*α), cassiterite (Sn Lα), synthetic $NiTa_2O_6$ (Ta *M*α), synthetic UO_2 (U *M*α), synthetic ThO_2 (Th *M*α), galena (Pb *M*β), hafnon (Hf *M*α), apatite (P *K*α), and synthetic $CoWO_4$ (W *M*α). Count times for all elements except F were 20 seconds on peak, and 10 seconds on background. Count times for F were 50 seconds on peak and 25 seconds on background. Raw intensities were corrected using the PAP routine (Pouchou & Pichoir 1984). Table 2 contains EMPA data for pyrochlore supergroup minerals with formulae calculated on the anhydrous basis of two $^{[6]}B$-site cations (Nb+Ta,+Zr+ Hf+Ti+Fe^{3+}+Sn+W+Si+Al = 2 apfu) in accordance with the Atenico et al. (2010).

Powder X-ray diffraction

Powder X-ray diffraction data for each pyrochlore supergroup sample were acquired at the Canadian Museum of Nature X-ray Diffraction Laboratory using a Bruker AXS D8 Discover equipped with a Hi-Star 2D detector and operated with a GADDS system. The instrument was calibrated using the statistical approach described by Rowe (2009). Analyses were performed at 40kV and 40mA with Cu*K*α radiation and a sample-to-detector distance of 12 cm. All samples analysed are metamict and give only broad, potato-like peaks.

The pyrochlore supergroup

The pyrochlore supergroup displays an extraordinarily wide geochemical variability, including extensive non-stoichiometry. Pyrochlore supergroup minerals are cubic oxides ($Fd\bar{3}m$) with a ~ 10.4 Å and Z = 8 (Rouse et al. 1998). They have a general formula $A_{2-m}B_2X_{6-w}Y_{1-n}$, where A = large [8]-coordinated cations (Na, Ca, Sr, Pb, Y, REE, U, Th), vacancies (□) or H_2O, B = [6]-coordinated high field-strength (HFSE) cations (Nb, Ti, Ta, Sb, W), X = O, OH or F, and Y = OH, F, O, H_2O, □, K, Cs or Rb. The symbols m, w and n represent incomplete occupancies in the A, X and Y sites, respectively. Values of m range from 0 to 2, w = 0 – 0.7 and n = 0 – 1 (Atencio et al. 2010). Calculation of a chemical formula is done on the basis of 2 B cations pfu (Nb+Ta,+Zr+ Hf+Ti+Fe^{3+}+Sn+W+Si+Al = 2 apfu) as HFSE have been shown to be immobile during the alteration process and vacancies have not been found to occur in this site. The presence of high concentrations of SiO_2 (~ 10 wt.%) in altered pyrochlore supergroup mineral chemical analyses has been noted by many authors (Johan & Johan 1977; Uher et al. 1998; Chakhmouradian & Mitchell 2002; Bonazzi et al. 2006) and the role of Si in the structure, whether in the [6]-coordinated site, dispersed as an amorphous phase, or within metamictized regions, has been debated extensively by various authors. In LPC pyrochlore supergroup samples, Si has been included in the B site total but recognized that it is a result of post-metamictization alteration by late-stage, Si-bearing fluids and has not been used to name the species.

Five groups are recognized under the new nomenclature based on the dominant cation at the B site: pyrochlore (sensu stricto, Nb-dominant), betafite (Ti-dominant), microlite (Ta-dominant), roméite (Sb-dominant) and elsmoreite (W-dominant). These root names are further modified using the dominant species of the dominant valence at the *Y* site, and the dominant species of the dominant valence group at the *A* site (Atenico et al. 2010). For example, fluornatropyrochlore is the name for a pyrochlore group species which is F- and Na-dominant. Only 7 species are officially IMA-approved, whereas 20 additional species in the literature require complete descriptions in order to achieve valid species status (Atenico et al. 2010).

Alteration textures

Back-scattered electron images (BSEI) of all the samples reveal a wide range of alteration patterns. The majority of primary magmatic features have been overprinted by either primary or secondary alteration as defined by Lumpkin & Ewing (1995). Five main types of alteration are evident.

1. Unaltered grains with minimal penetrating, fracture-controlled alteration characterized by lower average Z (atomic number; e.g. LACP-23, Fig.3A). A unique feature in these samples is the presence of fission tracks adjacent to altered fractures (Fig. 3B). Using terminology defined by Lumpkin & Ewing (1995), fracture-controlled alteration can be considered secondary alteration. It is possible that in many cases, the apparently "unaltered" grain has actually experienced primary alteration, with the required large-scale intracrystalline diffusion or coupled dissolution-reprecipitation having reached completion and the original composition no longer detectable.

2. Complex, diffuse-zoned grains with penetrating, fracture-controlled secondary alteration (Lumpkin & Ewing 1995) characterized by lower average Z (e.g. LACP-01, Fig. 3C). Such grains may contain both primary compositions and compositions which have undergone primary alteration. Figure 3D (AOL-4) depicts a sample in which only a small area of the grain is of primary composition (bright in BSEI) and the surrounding darker BSEI areas have experienced primary alteration.

3. Unaltered grains with penetrating, fracture-controlled secondary alteration grading into highly altered regions which display a conchoidal "hydration front" with low average *Z* (e.g. LACP-08, Fig. 3E). Conchoidal regions represent metamictized pyrochlore material which has essentially been transformed to glass, has undergone shrinkage during metamictization and destruction of the crystalline structure, followed by late-stage hydration by meteoric and/or hydrothermal fluids. Post-metamictization alteration may be considered a 4th type of alteration in addition to those listed by Lumpkin & Ewing (1995).

4. Heavily altered grains with an intense network or mosaic of fracture-controlled, secondary alteration (e.g. LACP-41, Fig. 3F).

5. Heavily altered grains with crystallographically-controlled (cubic) secondary alteration (e.g. LACP-32B, Fig. 3G). Alteration is controlled by the {111} cleavage of the pyrochlore structure and is reminiscent of exsolution observed in Fe-Ti-oxide phases.

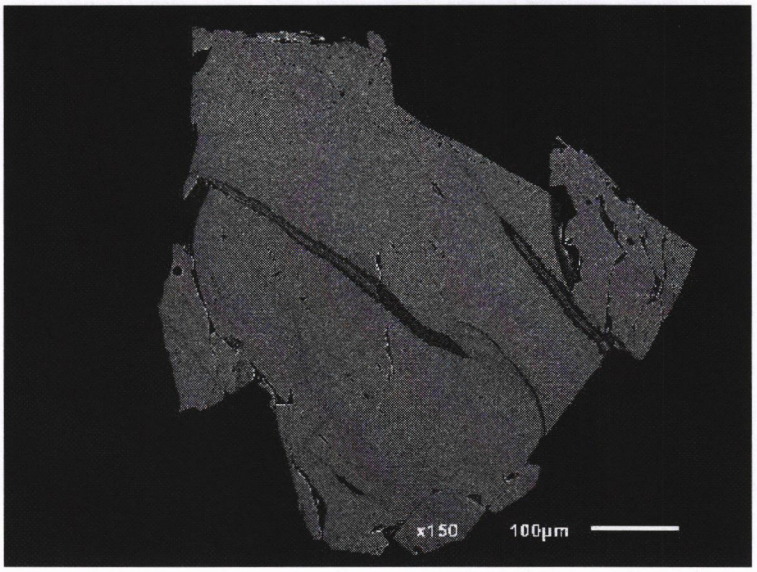

Fig. 3A. Fracture-controlled secondary alteration (LACP-23).
Torstein

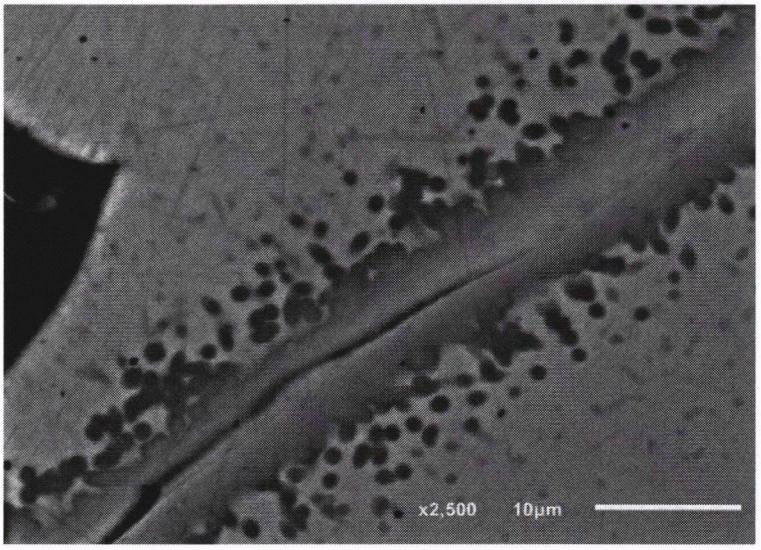

Fig. 3B. Alpha recoil damage in pyrochlore (LACP-23).

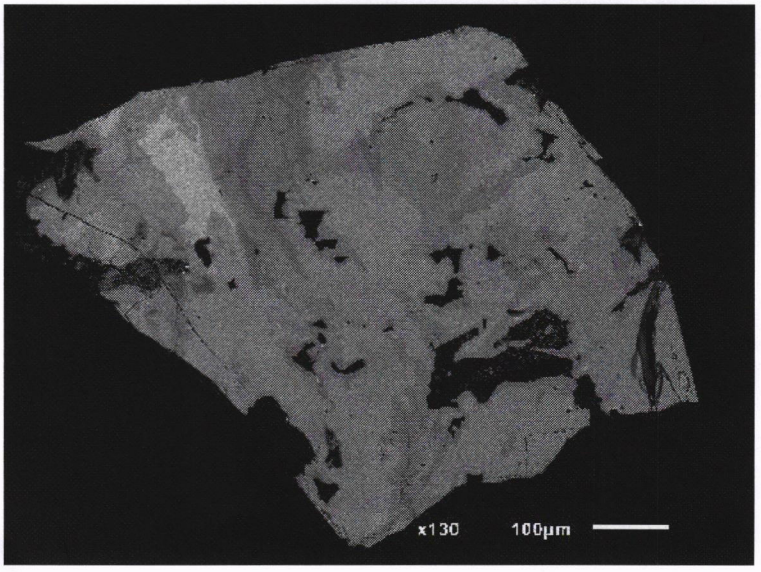

Fig. 3C. Primary and secondary alteration (LACP-01).
Almenningen

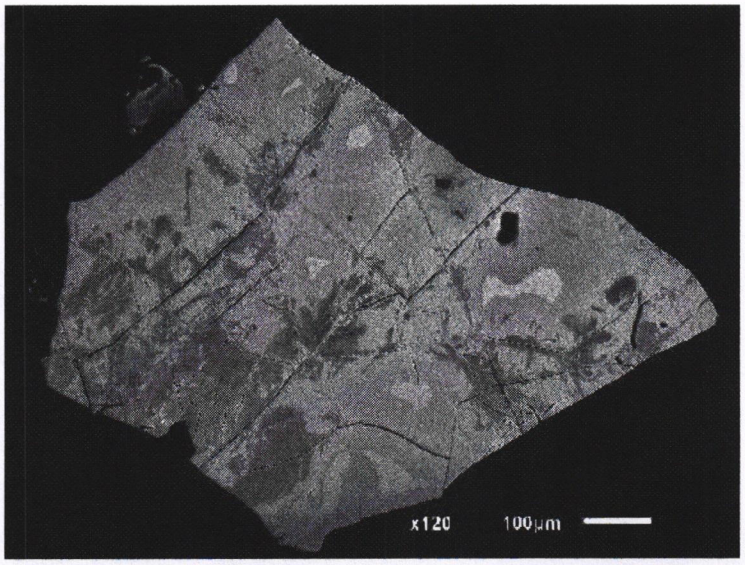

Fig. 3D. Primary and secondary alteration (AOL-4).

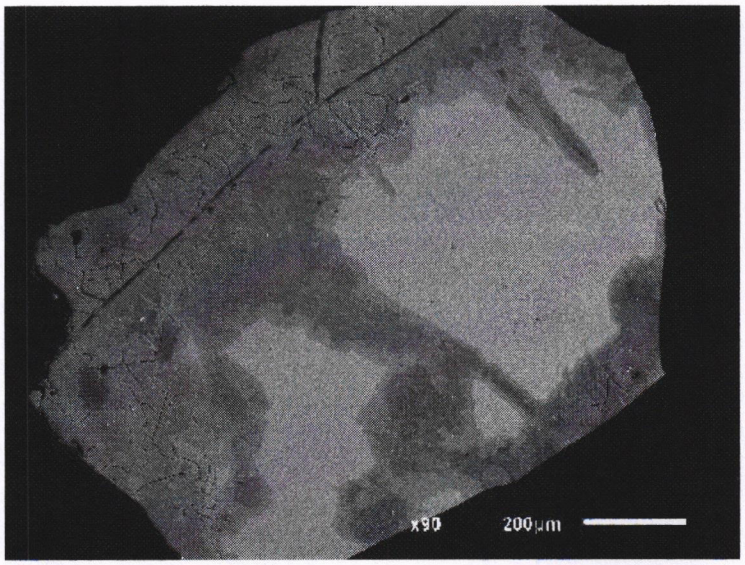

Fig. 3E. Secondary and post-metamictization alteration and hydration (LACP-08). Tuften

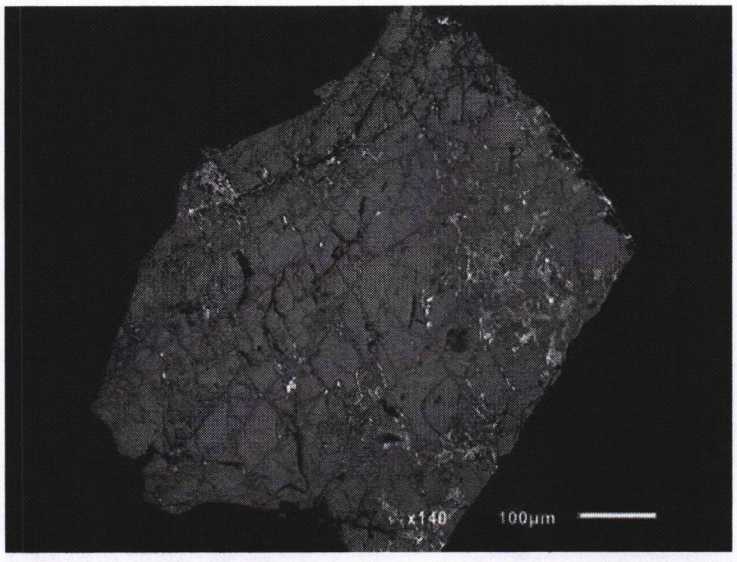

Fig. 3F. Extensive secondary alteration (mosaic; LACP-41).